International Journal of Recent Development in Engineering and Technology
Website: www.ijrdet.com (ISSN 2347-6435(Online) Volume 3, Issue 1, July 2014)

Upconversion Luminescence in Er^{3+} / Yb^{3+} Codoped Lead Bismuth Indium Borate Glasses

Y Raja Rao[1], K Krishnamurthy Goud[2], E Ramesh Kumar[3], M Chandra Shekhar Reddy[4], B Appa Rao[5]
Department of Physics, Osmania University, Hyderabad-500 007, India.

***Abstract*— The effect of Er^{3+} concentration on red emission in Er^{3+}/Yb^{3+}co-doped PbO-B_2O_3-Bi_2O_3-In_2O_3 glasses is reported. Optical absorption, FTIR and luminescence spectra of all the glasses were recorded at room temperature. The optical absorption spectra exhibited a band at 990nm due to transitions from the ground state $^4I_{15/2}$ and $^2F_{7/2}$ to excited states of Er^{3+} and Yb^{3+} ions, respectively. The other absorption bands at 491 nm ($^4F_{7/2}$), 523 nm ($^2H_{11/2}$), 565 nm ($^4S_{3/2}$), 660 nm ($^4F_{9/2}$), 812 nm ($^4I_{9/2}$) and 1525 nm ($^4I_{13/2}$) are attributed to transitions from the ground state $^4I_{15/2}$ to excited state of Er^{3+}. From the optical absorption spectra, optical band gap E_{opt}, Urbach energy values were calculated and it was observed that the E_{opt} decreases with increasing the concentration of Er^{3+} ions upto 0.6 mol% and increases with further increase in the concentration of Er^{3+} ions. The FT-IR data revealed the presence of BiO_3, PbO_4, BO_4 and BO_3 functional groups in all the investigated glasses. Green and red up-conversion emissions centered at 529, 542 and 656 nm corresponding to $^2H_{11/2} \rightarrow {}^4I_{15/2}$, $^4S_{3/2} \rightarrow {}^4I_{15/2}$ and $^4F_{9/2} \rightarrow {}^4I_{15/2}$ transitions, respectively, of Er^{3+} ions have been obtained under 980 nm laser excitation at room temperature. The results obtained are discussed quantitatively based on the energy transfer between Yb^{3+} and Er^{3+} ions.**

***Keywords*—Glasses, FTIR, Optical absorption, Photo luminescence, Rare earths.**

I. INTRODUCTION

In recent years upconversion luminescence has attracted many researches due their potential applications in optoelectronics such as in lasers, display, waveguide and imaging [1]. Now-a-days, more effort has been devoted for preparing the new upconversion materials and to study their emission properties. The efficiency of upconversion mainly depends on the phonon of the host materials. The higher phonon energy of the host material always leads to lower upconversion efficiency of rare earth ions [2]. Heavy metal oxide glasses are identified to have low phonon energy when compared with conventional oxide glasses such as silicate and phosphate glasses. These glasses have attracted attention of several researchers for excellent infrared transmission compared with the conventional glasses.

Attempts have been made to explore the mechanical, thermal and optical properties of these glasses. Among the other heavy metal oxide glasses, bismuth oxide glasses have wide range of applications in the field of glass ceramics, layers for optical and electronic devices, thermal and mechanical sensors, reflecting windows [3, 4].

Indium oxide participates in the glass network as network modifier and also as network former. With the addition of In_2O_3, transparency increases [5, 6]. Er^{3+} is the most popular and most efficient luminescent ion when compared with other rare earth ions. By using Yb^{3+} as a sensitizer, improves the energy transfer to Er^{3+} ions and luminescence efficiency. Generally upconversion is difficult to observe in glasses with phonon energies above 1000 cm^{-1}. With the addition of Yb^{3+} ions as a sensitizer it is possible to observe the upconversion luminescence [7].

Er^{3+}, ions are well known due to their effective blue, green and red emissions and also due to the near infrared emission at ~2.0 μm. Additionally these ions are well recognized due to their up−conversion of infrared to visible light [8]. Er^{3+} ions possess strong infrared emission transition viz., $^4I_{13/2} \rightarrow {}^4I_{15/2}$. However, in the conventional oxide host glass matrices this transition is disturbed by significant multi-phonon deexcitation due to the presence of high phonon energy contribution of glass formers, favoring effective losses due to non-radiative transitions. Such losses can be minimized, if the glasses are co-doped with another rare earth ion like Yb^{3+}.

The ground state of trivalent ytterbium ion (Yb^{3+}) is $^2F_{7/2}$. The doublet splitting of this state is approximately 10,000 cm^{-1} with the $^2F_{5/2}$ component lying above the ground state, $^2F_{7/2}$, with the average radiative lifetime ~ 0.28 ms. Yb^{3+} ion is reported to act as a donor or alternately as an energy transfer bridging ion between a donor and an acceptor ion in several glass systems [9]. In particular, this ion is considered as a promising sensitizer for Er^{3+} ions in glass matrices, due to its significantly high absorption cross section in the NIR region and favourable energy level structure.

International Journal of Recent Development in Engineering and Technology
Website: www.ijrdet.com (ISSN 2347-6435(Online) Volume 3, Issue 1, July 2014)

In fact, efficient energy transfer processes from Yb^{3+} to Er^{3+} ions [19] when excited at 980 nm (corresponding to $^2F_{7/2} \rightarrow {}^2F_{5/2}$ transition of Yb^{3+} ion) intense R, G and B emissions were expected in different kinds of glass matrices [10]. In this paper we have investigated the reinforcement of red emission transition of Er^{3+} ions due to Yb^{3+} co-doping in $PbO\text{-}B_2O_3\text{-}Bi_2O_3\text{-}In_2O_3$ glass system when excited by 980 nm semiconductor laser.

As a part of studying the upconversion phenomenon of Er^{3+} / Yb^{3+} co-doped glasses in different host glasses, we have already reported upconversion in $PbO\text{-}B_2O_3\text{-}Bi_2O_3\text{-}Al_2O_3$ and $PbO\text{-}B_2O_3\text{-}Bi_2O_3\text{-}Ga_2O_3$ glass systems [11, 12].

II. Experimental

For the present study, glasses of composition $[100\text{-}(x+y)][0.5PbO\text{-}0.25B_2O_3\text{-}0.20Bi_2O_3\text{-}0.05In_2O_3]\text{-}xEr_2O_3\text{-}yYb_2O_3$ with y = 0 for x = 0, 0.2; y = 0.2 for x =0 to 1.0 (step 0.2) are chosen and the glasses are labeled as IE0Y0, IE2Y0, IE0Y2, IE2Y2, IE4Y2, IE6Y2, IE8Y2 and IE10Y2 respectively. Appropriate amounts of AR grade reagents of PbO, B_2O_3, Bi_2O_3, In_2O_3, Er_2O_3 and Yb_2O_3 powders are thoroughly mixed in agate mortar and melted in a porcelain crucible in the temperature range of 900 to 950°C in a programmable electrical furnace for thirty minutes until bubble free liquid is formed. The resultant melt is poured in a brass mould and subsequently annealed at 250°C for 2h. The samples prepared were then ground and optically polished to the dimensions of 1 cm × 1 cm × 0.2 cm in order to meet the requirements for optical measurements.

X-ray diffraction analysis was carried out using Rigaku miniflex X-ray diffractometer. The absorption spectra were obtained with the JASCO Model V-670 UV–VIS–NIR spectrophotometer from 400–1700 nm with a spectral resolution of 0.1 nm. Infrared transmission spectra were recorded on a Bruker FT-IR–TENSOR27 spectrophotometer up to a resolution of 0.4 cm^{-1} in the spectral range 400–2000 cm^{-1} using potassium bromide pellets (300 mg) containing pulverized sample (1.5 mg). The luminescence spectra were recorded at ambient temperature using JOBIN YVON Fluorolog-3 spectrofluorometer.

The density (ρ) of the glass samples at room temperature was measured to an accuracy of ±0.01g/cm^3 by using Archimedes principle.

From the values of density and average molecular weight of the samples (M), various physical parameters like molar volume, oxygen packing density, Er^{3+} and Yb^{3+} ion concentrations (Ni), interionic distance (r_i) and polaron radius (r_p) were calculated using standard equations [13] and are presented in Table I.

III. Results And Discussion

A. X-ray Diffraction

The absence of the sharp peaks in the X-ray diffraction pattern (Fig. 1) confirms the amorphous nature of the glass samples.

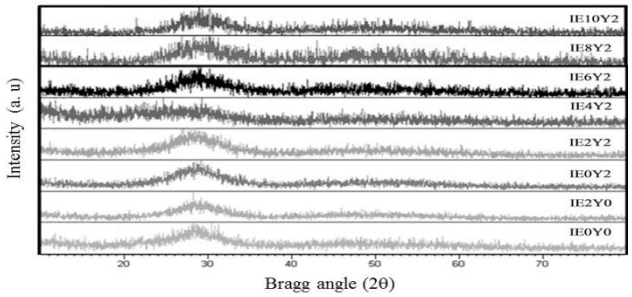

Fig. 1 X-Ray diffraction patterns of IEY glass system

B. Optical Absorption and J-O Analysis

Fig. 2 shows the absorption spectra of Er^{3+} / Yb^{3+} co-doped glass samples. The absorption band centered at 990 nm is attributed to transitions from the ground state $^4I_{15/2}$ and $^2F_{7/2}$ to excited states of Er^{3+} and Yb^{3+} respectively. The other absorption bands centered at 491nm($^4F_{7/2}$), 523 nm ($^2H_{11/2}$), 565 nm ($^4S_{3/2}$), 660 nm ($^4F_{9/2}$), 812 nm ($^4I_{9/2}$) and 1525 nm ($^4I_{13/2}$) are attributed to transitions from the ground state $^4I_{15/2}$ to excited state of Er^{3+} [14]. The intensities of these spectral bands are found to increase with the increase of Er^{3+} concentration and no significant shift is observed in the position of the bands. From Fig. 2 it can be seen that the absorption edge shifts towards longer wavelength side with doping of the rare earth ions.

From Fig. 2 it can also be seen that, for all the glasses, there is an exponential rise of absorption towards the edge. In all the cases edges are sharply defined. The absorption coefficient α(ω) below and near the fundamental absorption edge of each curve in Fig. 2 was determined using the relation [15].

International Journal of Recent Development in Engineering and Technology
Website: www.ijrdet.com (ISSN 2347-6435(Online) Volume 3, Issue 1, July 2014)

TABLE I
VARIOUS PHYSICAL PARAMETERS OF IEY GLASS SYSTEM

Physical parameter	IE0Y0	IE0Y2	IE2Y0	IE2Y2	IE4Y2	IE6Y2	IE8Y2	IE10Y2
Avg. molecular weight, M (g/mol)	236.07	236.39	236.37	236.68	236.97	237.27	237.56	237.85
Density, ρ (g/cm^3) (±0.001)	7.031	7.098	7.056	7.123	7.148	7.173	7.198	7.223
Oxygen packing density, O (g atom/L)	0.0595	0.0601	0.597	0.0603	0.0605	0.0607	0.0609	0.0610
Er ion concentaration, N_i (x10^{21}/cc) (±0.001)	0	0	0.107	0.108	0.218	0.327	0.437	0.548
Molar Volume, V_m (cc/mol) (±0.01)	33.57	33.30	33.49	33.22	33.15	33.07	33.00	32.98
Er Inter ionic distance, r_i (Å) (±0.01)	-	-	21.00	21.00	16.61	14.50	13.16	12.21
Polaran radius of Er, r_p (Å) (±0.01)	-	-	13.43	13.43	10.62	9.27	8.42	7.81
Yb ion concentaration, N_i (x10^{21}/cc) (±0.001)	0	0.108	0	0.108	0.108	0.108	0.108	0.108
Yb Inter ionic distance, r_i (Å) (±0.01)	-	20.96	-	20.96	20.96	20.96	20.96	20.96
Polaran radius of Yb, r_p (Å) (±0.01)	-	13.41	-	13.41	13.41	13.41	13.41	13.41

$$\alpha(\omega)=(1/t)\ln(I/I_0) \qquad (1)$$

Where 't' is the thickness of each sample and $\ln(I/I_0)$ corresponds to absorbance. Thus data for Fig.3 were obtained from the relation [15]:

$$\alpha(\omega) = \text{const.}\ (\hbar\omega - E_{opt})^2/\hbar\omega \qquad (2)$$

Where E_{opt} is the energy of the optical band gap, and $\hbar\omega$ is the photon energy of the incident radiation. Since relation (2) can be rearranged to represent the linearity between $(\alpha\hbar\omega)^{1/2}$ and $(\hbar\omega - E_{opt})$ as

$$(\alpha\hbar\omega)^{1/2} = const(\hbar\omega - E_{opt}) \qquad (3)$$

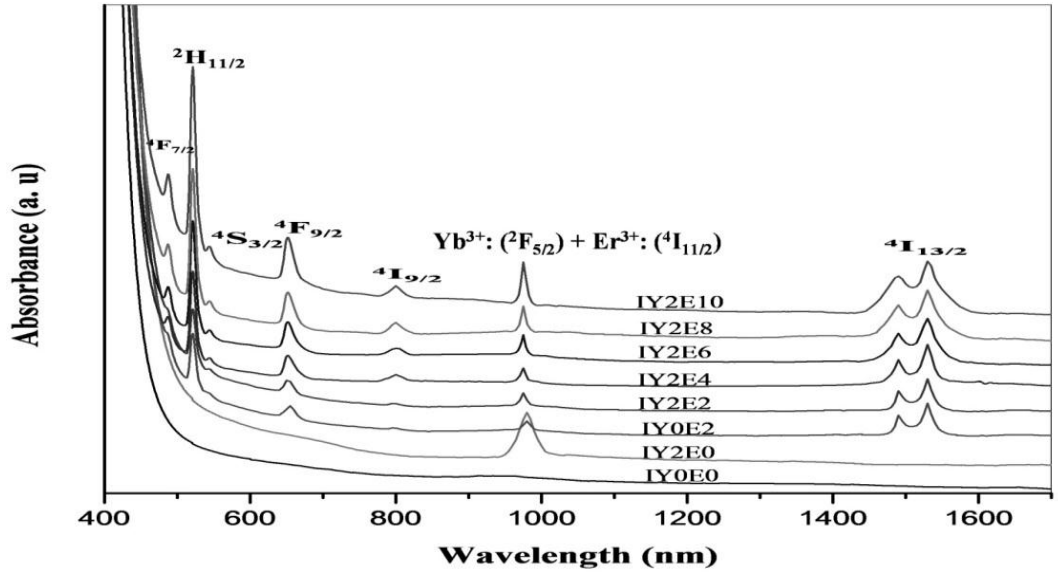

Fig. 2 Optical absorption spectra of IEY glass system

International Journal of Recent Development in Engineering and Technology
Website: www.ijrdet.com (ISSN 2347-6435(Online) Volume 3, Issue 1, July 2014)

One can determine the optical band gap values from the curves representing $(\alpha\hbar\omega)^{1/2}$ as a function of the photon energy ($\hbar\omega$) (Fig. 3). Thus the data obtained from Fig. 2 is fitted to equation (3) for linear regions of curves in Fig. 3 by the method of least squares.

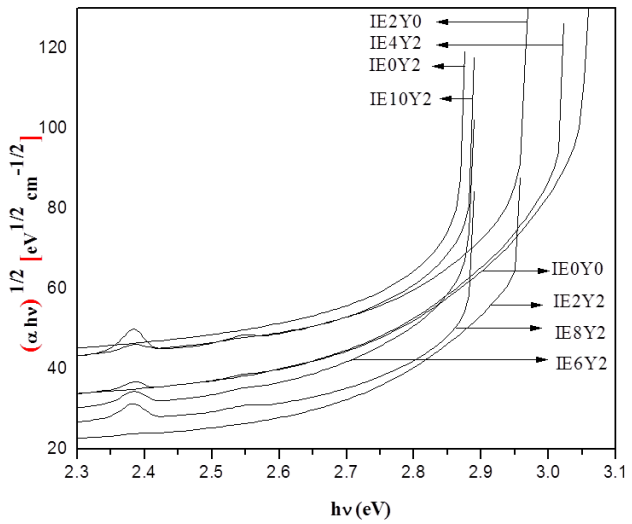

Fig. 3 The $(\alpha h\nu)^{1/2}$ as a function of photon energy for the IEY glass system.

The E_{opt} values were determined from the curves representing $(\alpha\hbar\omega)^{1/2}$ as a function of photon energy $(\hbar\omega)$ by extrapolation of the linear region of the plots to $(\alpha\hbar\omega)^{1/2} = 0$. The logarithm of the absorption coefficient was plotted as a function of photon energy. The values of Urbach energies (ΔE) were calculated by taking the reciprocals of the slopes of the linear portion in the lower photon energy region of these curves. The values of E_{opt} and Urbach energy values are presented in Table II.

From the optical absorption spectra it is observed that the cut-off wavelength shifts towards longer wavelength side with doping of rare earth ions. From the spectra it was observed that with increasing the concentration of Er^{3+}, keeping Yb^{3+} constant (0.2 mol %), cut-off wavelength shifts towards longer wavelength side resulting the decrease in the value of E_{opt}. Further increasing the concentration of Er^{3+} ions, cut-off wavelength shifts towards lower wavelength side and E_{opt} value increases.

The validity of the Eq. (2) between ($\hbar\omega$ $^{1/2}$ and $\hbar\omega$, points out that the optical band gap is caused by amorphous optical absorption edge.

This indicates the fact that the disordered amorphous glass materials have prevailingly the direct transitions between the valence band and the conduction band and the absence of the indirect inter-band transitions like in the case of the crystals (i.e. the transitions in the different points of the Brillouin zone). Some deviations observed from this dependence are understood due to trapping of some disordered states within the energy gap.

TABLE II
CUT-OFF WAVELENGTH, OPTICAL BAND GAP AND URBACH ENERGY OF IEY GLASS SYSTEM

S.No.	Sample code	Cut-off wavelength (nm)	E_{opt} (eV) ±0.01	ΔE (eV) ±0.001
1	IE0Y0	410	3.04	0.255
2	IE2Y0	422	2.93	0.197
3	IE0Y2	434	2.86	0.245
4	IE2Y2	424	2.94	0.186
5	IE4Y2	419	2.99	0.219
6	IE6Y2	413	3.01	0.214
7	IE8Y2	427	2.88	0.225
8	IE10Y2	432	2.81	0.276

We have also observed an increase in the optical band gap with the increase in the concentration of Er_2O_3 up to 0.6 mol% (Table 2) suggests decreasing degree of depolymerization or concentration of bonding defects and non-bridging oxygens (NBO) in the glass network up to this concentration of Er_2O_3.

The Judd-Ofelt parameters Ω_2, Ω_4 and Ω_6 [16] can be determined by obtaining the experimental ground state oscillator strengths of the absorption transitions via an integration of the absorption coefficients for each band according to the following equation

$$f_{\exp} = \frac{mc^2}{\pi e^2 N_0}\int \varepsilon(\upsilon)d\upsilon \qquad (4)$$

Where ε(ν) is the absorption coefficient, ν is the energy (cm^{-1}) of the transition and N_0 is the density of the ions (cm^{-3}). The measured line strength is used to calculate the intensity parameters Ω_2, Ω_4 and Ω_6 by solving a set of equations for the corresponding transitions between initial $|(S,L)J\rangle$ and terminal $|(S',L')J'\rangle$ manifolds expressed by [16]

International Journal of Recent Development in Engineering and Technology
Website: www.ijrdet.com (ISSN 2347-6435(Online) Volume 3, Issue 1, July 2014)

$$f_{theo}(JJ') = \frac{8\pi^2 mcv}{3h\,(2J+1)e^2}\,[\chi\, S_{ed}(JJ') + nS_{md}(JJ')] \qquad (5)$$

Where $\chi = (n^2+2)^2/9n$ is a factor for the effective field at the well-localized center in a medium of isotropic refractive index n and S_{ed} and S_{md} are the electric dipole and magnetic dipole line strengths respectively. All the spectra of rare earth ions arise from intraconfiguration transitions within the 4f shell [16] which are forbidden by the parity rule of electric dipole transitions.

However, ions incorporated in a host matrix can experience a non-centro symmetric crystal field interaction. This interaction admixes the states of opposite parity, thereby relaxing the parity restrictions [16]. Their contribution is then given by

$$S_{ed}(JJ') = e^2 \Sigma \Omega_\lambda \,|\langle (SL)J \,|\, U^\lambda \,|\, (S'L')J'\rangle|^2 \qquad (6)$$

The selection rules for the electric dipole contribution S_{ed} from the *f*-configuration mixing include $\Delta l = \pm l, \Delta S = 0$, $|\Delta l|$ and $|\Delta l| \leq 6$. However, the magnetic dipole transitions are parity allowed between states of f'' and obey the selection rules $\Delta S = \Delta L = 0$, $\Delta J = 0$ *and* ± 1 (but not $0 \rightarrow 0$ transitions). Its contribution is given by the equation

$$S_{md}(JJ') = \left(\frac{eh}{8\pi^2 mc}\right)^2 |\langle (SL)J \| \mathbf{L} + 2\mathbf{S} \| (S'L')J'\rangle|^2 \qquad (7)$$

The values of the reduced matrix elements $\|U^{(\lambda)}\|^2$ and $\|\mathbf{L}+2\mathbf{S}\|^2$ were calculated by Carnall et al. and weber. The calculation of the parameters were performed minimizing the root mean square (rms) deviation of the measured and calculated oscillator strength, respectively

$$\delta_{rms} = \sqrt{\frac{\sum_{i=1}^{p}\left(f_{meas}^{(i)} - f_{theo}^{(i)}\right)^2}{p-3}} \qquad (8)$$

Where p is the number of absorption bands and 3 indicates the number of fitting parameters. From the phenomenological parameters Ω_2, Ω_4 and Ω_6, the radiative transition rates of all of the excited states of interest are calculated through the relation [16]

$$A_R(JJ') = \frac{64\pi^4}{3h\,(2J+1)\lambda^3}\,[\chi\, S_{ed}(JJ') + n^3 S_{md}(JJ')] \qquad (9)$$

The emission branching ratio for transitions originating from an initial manifold *i* can be obtained from the radiative transition probabilities using the following equation

$$\beta_r = \frac{A_{JJ'}^{i,j}}{\sum_j A_{JJ'}^{i,j}} = A_{JJ'}^{i,j}\tau_R \qquad (10)$$

Where τ_R is the radiative life time.

The Judd-Ofelt theory has often been used to calculate the spectroscopic parameters, such as predicted life time, oscillator strength and branching ratios (β_r) and the results are summarized in Table IV and Table V. It is well established that an emission level with β_r value above 50% becomes a potential laser emission [17]. Referring to the data on emission transitions in the present glass system, the transition $^4F_{9/2} \rightarrow {}^4I_{15/2}$ has the highest value of β_r among various transitions. This transition may therefore be considered as a possible laser transition.

TABLE III
EXPERIMENTAL AND CALCULATED OSCILLATOR STRENGTH VALUES OF Er^{3+} SINGLY DOPED GLASS

Transition from $^4I_{15/2}$ →	IE2Y0	
	$f_{exp}(10^{-6})$	$f_{cal}(10^{-6})$
$^4I_{13/2}$	2.8965	2.8963
$^4I_{11/2}$	1.3612	1.3427
$^4I_{9/2}$	0.3060	0.2938
$^4F_{9/2}$	3.0426	3.0401
$^4S_{3/2}$	1.2006	1.1886
$^2H_{11/2}$	8.8119	8.8133
$^4F_{7/2}$	4.0724	4.1048
r.m.s. deviation	±0.016	

TABLE IV
PREDICTED LIFE TIME AND BRANCHING RATIO OF Er^{3+} SINGLE DOPED GLASS

Transitions	IE2Y0	
	β_r (%)	$\tau_{R(ms)}$
$^2H_{11/2} \rightarrow {}^4I_{15/2}$	54	0.146
$^4S_{3/2} \rightarrow {}^4I_{15/2}$	55	0.229
$^4F_{9/2} \rightarrow {}^4I_{15/2}$	58	0.428

International Journal of Recent Development in Engineering and Technology
Website: www.ijrdet.com (ISSN 2347-6435(Online) Volume 3, Issue 1, July 2014)

The comparision of Judd-Ofelt parameters Ω_2, Ω_4 and Ω_6 of Er^{3+} in various hosts is presented in Table V. Ω_2 is related with the symmetry of the glass hosts while Ω_6 is inversely proportional to the covalency of Er-O bond. The Er-O bond is assumed to be dependent on the local basicity around the RE sites, which can be adjusted by the composition or structure of the glass hosts. From the values of Judd-Ofelt parameters it was observed that for the present glass $\Omega_2 > \Omega_4 > \Omega_6$.

TABLE V
J-O PARAMETERS OF Er^{3+} IN DIFFERENT GLASS HOSTS

Glasses	Ω_2 (10^{-20} cm^2)	Ω_4 (10^{-20} cm^2)	Ω_6 (10^{-20} cm^2)	Reference
IE2Y0	5.34	2.75	1.05	Present
Phosphate	6.65	1.52	1.11	19
Silicate	4.23	1.04	0.61	19
Germanate	5.81	0.85	0.28	19
Fluoride	2.91	1.27	1.11	19

C. FTIR Spectra

FTIR spectra in the range 4000-1600cm^{-1}, of IEY glasses doped with rare earth ions are shown in Fig. 4. The spectra of undoped glass sample exhibited a broad absorption band at 3424cm^{-1} and a weak band at 1640 cm^{-1}, which are mainly due to the presence of hydroxyl group and is attributed to O-H stretching vibration. With the addition of rare earth ions O-H content decreases and becomes completely invisible for higher concentration of rare earth ions. The OH absorption increases the optical attenuation and decreases quantum efficiency of the rare earth excited levels, as well as leads to the luminescence quenching and thereby decreases the utility of these materials for potential application such as ultra-low loss fibers. Hence a great effort is necessary for the synthesis of high quality glass with minimum OH content [18].

The IR spectrum of undoped glass sample exhibits two peaks at 2924cm^{-1} and 2854cm^{-1} which are attributed due to the presence of hydrogen bonding.

But in the case of doped samples the peak intensity decrease with increasing the concentration of rare earth ions and the peaks are completely invisible for the higher concentration of rare earth ions. This implies that the addition of rare earth ions reduces the number of hydrogen bonds [19].

Fig. 5 shows the FTIR spectra of IEY glasses doped with rare earth ions in the range 1600-400cm^{-1}. The spectra revealed the characteristic absorption bands for B_2O_3 and Bi_2O_3 of their various structural units. The IR spectra of the glasses containing Bi_2O_3 are expected to exhibit four fundamental vibrations at about 830 cm^{-1}, 620 cm^{-1}, 450 cm^{-1} and 350 cm^{-1}. B_2O_3 is also expected to exhibit three vibrational bands in the regions at (i)1200-1600 cm^{-1}, due to stretching vibrations of B-O bond of trigonal BO_3 units, (ii) 800-1200 cm^{-1}, due to B-O bond stretching of the tetrahedral BO_4 units and (iii) band around 700 cm^{-1}, due to the bending of B-O-B linkages in borate network. The band around ~490 cm^{-1}, is due to PbO_4 structural units and also due to symmetrical bending vibrations of BiO units [20-23]. The band positions and corresponding IR assignments presented in Table VI.

TABLE VI
ABSORPTION BANDS AND THEIR ASSIGNMENTS IN FT-IR SPECTRA

Wave number (cm^{-1})	IR assignments
~490-500	Bending vibrations of Bi_2O_3 pyramidal units, Pb-O-B bending vibrations.
~705-710	Vibrations of B-O-B linkages
~895-918	Asymmetric stretching vibrations of B-O bands in BO_4 units
~1213-1274	Asymmetric stretching modes of borate triangles BO_3 and BO_2O^-
~1640	O-H stretching vibration
~2853, ~2923	Presence of hydrogen bonding
~3424	O-H stretching vibration

As the concentration of Er_2O_3 is increased upto 0.6 mol%, the intensity of the band due to BO_4 structural units is observed to increase and when the concentration of Er_2O_3 is raised beyond 0.6 mol% the band due to BO_3 structural units is observed to grow at the expense of the band due to BO_4 structural units.

International Journal of Recent Development in Engineering and Technology
Website: www.ijrdet.com (ISSN 2347-6435(Online) Volume 3, Issue 1, July 2014)

D. Upconversion Spectra

The room temperature upconversion spectra of Er^{3+}/Yb^{3+} co-doped [100-(x+y)][0.5PbO-0.25B_2O_3-0.20Bi_2O_3-0.05In_2O_3]-$x$$Er_2O_3$-$y$$Yb_2O_3$ glasses under 980nm excitation are shown in Fig. 4. The emission spectra of the co-doped glasses excited at 980 nm exhibited the bands due to the following emission transitions between $^2H_{11/2} \rightarrow {}^4I_{15/2}$ (Green) , $^4S_{3/2} \rightarrow {}^4I_{15/2}$ (Green) , $^4F_{9/2} \rightarrow {}^4I_{15/2}$ (Red) due to Er^{3+} ions [2]. As the concentration of Er_2O_3 is increased beyond 0.6 mol% the red emission band is observed to grow gradually.

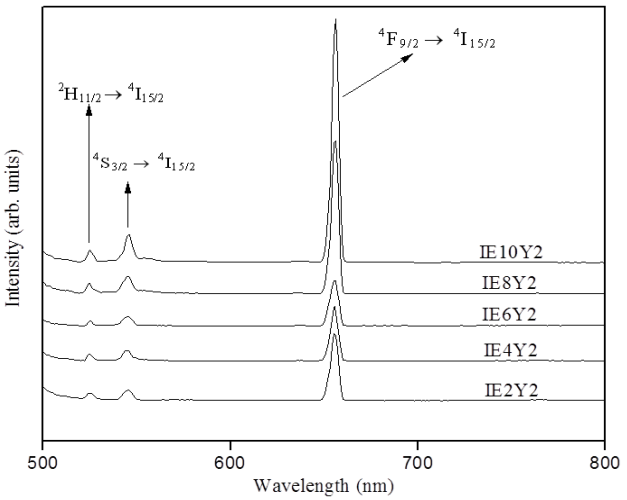

Fig. 4 Upconversion fluorescence spectra of IEY glass system at room temperature.

This is due to the fact that In^{3+} ions (like any other III A group elemental ions), isolate the rare-earth ions from RE-O-RE bonds and form In-O-RE bonds. Such declustering effect which seems to be dominant in the glasses containing higher concentrations of Er_2O_3, leads to the larger spacing between RE ions and contributes for the enhancement of fluorescence emission.

Under 980 nm excitation, Er^{3+} ions get excited from ground state ($^4I_{15/2}$) to excited state ($^4I_{11/2}$) due to (i) ground state absorption (ii) phonon assisted energy transfer from Yb^{3+} and (iii) energy transfer from the $^4I_{11/2}$ state of adjacent Er^{3+}. Due to larger absorption cross section of Yb^{3+}, at around 980 nm, phonon assisted energy transfer from Yb^{3+} is the dominant one.

When $^4I_{11/2}$ state becomes more populated, the ions in that state are promoted to the $^4F_{7/2}$ state due to any one of the following methods: (i) excited state absorption (ii) phonon assisted energy transfer from Yb^{3+} and (iii) energy transfer from the $^4I_{11/2}$ state of adjacent Er^{3+}. By following any one of the above processes $^4F_{7/2}$ state becomes populated.

The Er^{3+} ions in the populated $^4F_{7/2}$ state, makes transition to the intermediate state $^2H_{11/2}$ ($^4S_{3/2}$) due to multiphonon relaxation process. This transition is non-radiative and very fast. Now Er^{3+} ions in the $^2H_{11/2}$ and $^4S_{3/2}$ states, give rise to green emission due to $^2H_{11/2} \rightarrow {}^4I_{15/2}$ (525 nm) and $^4S_{3/2} \rightarrow {}^4I_{15/2}$ (542 nm) transition. The Er^{3+} ions in the populated state $^4I_{11/2}$, can also make transition to metastable state $^4I_{13/2}$ due to multiphonon relaxation process. This transition is non-radiative.

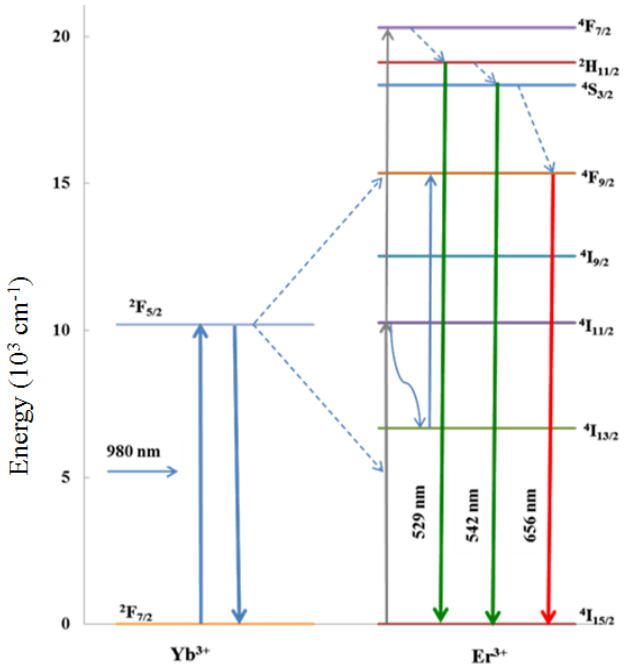

Fig. 5 Schematic illustration of the upconversion mechanism in IEY glasses [24, 25]

By following any one of the following processes the ions in the $^4I_{13/2}$ state are promoted to $^4F_{9/2}$ state. (i) Excited state absorption (ii) Phonon assisted energy transfer (iii) Energy transfer from the $^4I_{11/2}$ state of adjacent Er^{3+} and also (iv) Contribution from higher energy state $^4S_{3/2}$ through a non-radiative process.

International Journal of Recent Development in Engineering and Technology
Website: www.ijrdet.com (ISSN 2347-6435(Online) Volume 3, Issue 1, July 2014)

Now the transition from $^4F_{9/2}$ state to $^4I_{15/2}$ state gives red emission at 656nm [1, 24, 25]. In addition to the de-clustering influence of Er^{3+} ions by In^{3+} ions mentioned earlier. This type of energy transfer due to cross-relaxation enhances the intensity of the red emission in the studied glasses.

The upconversion mechanisms of Er^{3+}/Yb^{3+} ions are shown in Fig. 5. In the upconversion mechanisms of Er^{3+} ions, excited state absorption and energy transfer are the dominant processes. Excited state absorption is a single ion process and independent of the ion concentration in the glass. Energy transfer process depends on the concentration of Er^{3+} ions and this process rarely occurs between the excited ions, when the concentration of Er^{3+} is low. Upconversion luminescence intensities of red emission as a function Er_2O_3 concentration at fixed Yb_2O_3 (0.2 mol%) is shown in Fig. 6.

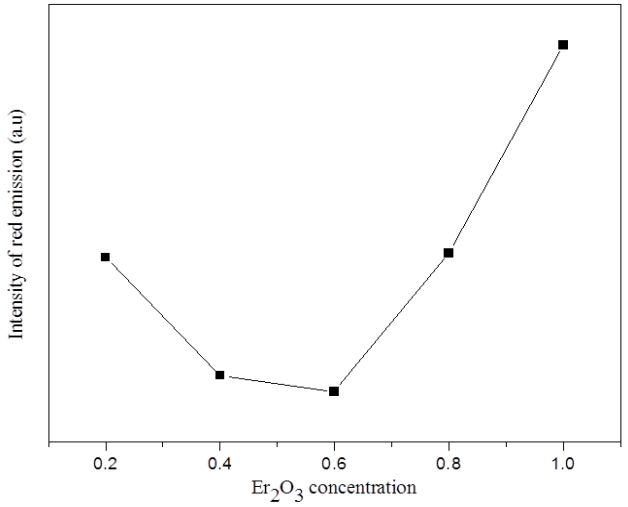

Fig. 6 Upconversion luminescence red intensity as a function of Er_2O_3 concentration at fixed Yb_2O_3 (0.2 mol%)

IV. CONCLUSIONS

X-ray diffraction studies have confirmed the amorphous nature of the materials prepared. From the optical absorption spectra it was observed that the E_{opt} decreases with increasing the concentration of Er^{3+} ions upto 0.6 mol% and increases for further increase in the concentration of Er^{3+} ions. From the values of Judd-Ofelt parameters it is observed that for the present glass system $\Omega_2 > \Omega_4 > \Omega_6$.

The value of Ω_2 which is related to the structural changes in the vicinity of the Er^{3+} ion indicates the highest covalent environment of Er^{3+} ion in IEY glasses and the value is greater than the fluoride and silicate glasses. The radiative transition probabilities and branching ratios evaluated for various luminescent transitions observed in the luminescence spectra suggests the highest value for $^4F_{9/2} \rightarrow {}^4I_{15/2}$ transition. The FT-IR spectra of these glasses exhibited the bands due to BiO_3, PbO_4, BO_4 and BO_3 functional groups in all the glasses investigated. The analysis of these studies has revealed an increasing degree of disorder in the glass network when the concentration of Er_2O_3 is greater than 0.6 mol%.

Green and red up-conversion emissions centered at 529, 542 and 656 nm corresponding to $^2H_{11/2} \rightarrow {}^4I_{15/2}$, $^4S_{3/2} \rightarrow {}^4I_{15/2}$ and $^4F_{9/2} \rightarrow {}^4I_{15/2}$ transitions of Er^{3+} ions have been obtained under the excitation of 980 nm laser radiation at room temperature. The green emission is very weak and the red emission is very prominent. From the emission spectra it was observed that the intensity of red emission increases with increasing the concentration of Er_2O_3 beyond 0.6 mol%. Such increase is attributed to i) the upconversion or the energy transfer from the emission transition of Yb^{3+} ion to Er^{3+} ions and ii) due to the declustrization of Er^{3+} ions by In^{3+} ions which may decrease the quenching of the luminescence.

Acknowledges

One of the authors (Y. Raja Rao) thankful to UGC, New Delhi for awarding FDP. The authors are also thankful to OU-DST-PURSE program for financial support.

REFERENCES

[1] Minghui Zhang, YanLiu, Jianding Yu, Xiuhong Pan, Shinchi Yoda. A novel upconversion TiO_2-La_2O_3-Ta_2O_5 bulk glass co-doped with Er^{3+}/Yb^{3+} fabricated by containerless processing. Materials letters, 2012, 66, 367-369.

[2] Yang Kuisheng, Xue Huili, Wu Rinang, Kan Jiaqiang, Wang Weizhong, Zeng Bin, Zhang Xiyan. Research on Up-conversion Mechanism in Er^{3+}/Yb^{3+} -codoped Oxyfluoride Glass J. of Rare Earths, 2006, 24, 175.

[3] Sudhakar K S V, Satyanarayana T, Srinivasa RaoL, Srinivasa Reddy N and Veeraiah N. Optical absorption and self activated pconversion fluorescence spectra of Tm^{3+} ions in antimony borate glass system. Solid State Communications, 2008,146, 441-445.

[4] Shiv Prakash Singh, Chakradhar R P S, Rao J L and Basudeb Karmakar. EPR, FTIR, Optical absorption and photoluminescence studies of Fe_2O_3 and CeO_2 doped ZnO-Bi_2O_3-B_2O_3 glasses. J. of Alloys and Compounds, 2010, 493, 256-262.

[5] Srinivasa Reddy M, Naga Raju G, Nagarjuna G, Veeraiah N. Structural influence of aluminium, gallium and indium metal oxides by means of dielectric and spectroscopic properties of $CaO–Sb_2O_3$ – B_2O_3 glass system. J. of Alloys and Compounds, 2007, 438, 41-51.

[6] Sahaya Baskaran G, Little Flower G, Krishna Rao D and Veeraiah N.Structural role of In_2O_3 in $PbO-P_2O_5-As_2O_3$ glass system by means of spectroscopic and dielectric studies. J. of Alloys and Compounds, 2007, 431, 303-312.

[7] Bomfim F A, Martinelli J R, Kassab L R P, Wetter N U, Neto J J. Effect of the ytterbium concentration on the upconversion luminescence of Yb3+/Er3+ co-doped $PbO-GeO_2-Ga_2O_3$ glasses. J. of Non-Crystalline Solids, 2008, 354, 4755-4759.

[8] Raghava Rao P, Venkatramaiah N, Gandhi Y, Ravi Kumar V, Kityk I V and Veeraiah N. Role of modifier oxide in emission spectra and kinetics of Er-Ho codoped $Na_2SO_4-MO-P_2O_5$ glasses. Spectrochimica Acta Part A, 2012, 86, 472-480.

[9] Purnachand N, Satyanarayana T, Kityk I V, Veeraiah N. Fluorescence studies of Yb3+ ions in lead antimony borate glass-Influence of crystallization. J. Alloys and Compounds, 2010, 492, 706-711.

[10] Li Feng, Boyuan Lai, Jing Wang, Guogiang Du, Qiang Su. Spectroscopic properties of Er^{3+} in a oxyfluoride glass and upconversion and temperature sensor behaviour of Er^{3+} / Yb^{3+} codoped oxyfluoride glass. J. Luminescence, 2010, 130, 2418-2423.

[11] Raja Rao Y, Krishnamurthy Goud K, Srinivas M and Appa Rao B. Spectroscopic properties of Er^{3+} and upconversion luminescence in Er^{3+}/Yb^{3+} codoped lead bismuth alumina borate glasses. Int. J. of Luminescence and its Applications, 2013, 32(Special issue), 170-173.

[12] Raja Rao Y, Krishnamurthy Goud K and Appa Rao B. Luminescence studies of $PbO-Bi_2O_3-Ga_2O_3-B_2O_3$ glasses doped with Er^{3+} / Yb^{3+}. AIP Conf. Proc., 2013, 1536, 661- 662.

[13] Reddy M C S, Appa Rao B, Brik M G, Prabhakar Reddy A, RaghavaRao P, Jayasankar C K and Veeraiah N. Emission charactersitics of Dy^{3+} ions in lead antimony borate glasses. Applied Physics B, 2012, 108(2), 455-461.

[14] SUN Hong-Tao, DAI Shi-Xun, XU Shi-Qing, HU Li-LI and JIANG Zhong-Hong. Frequency Upconversion Emission of Er^{3+} -Doped Strontium-Lead-Bismuth Glasses. CHIN.PHYS.LETT., 2004, 21, 2292-2294.

[15] Salagram M, Krishna Prasad V and Subrahmanyam K. Optical band gap studies on $xPb_3O_4-(1-x)P_2O_5$ lead [(II, IV0] phosphate glasses, Optical Materials, 2002, 18, 367-372.

[16] Taisa B.Brito, Vermelho M V D, Gouveia E A, and de Araujo M T. Optical characterization of Nd^{3+} and Er^{3+} doped lead-indium-phosphate glasses. J. of Applied Physics, 2007, 102,043113.

[17] Subbalakshmi P and Veeraiah N. Optical absorption and fluorescence properties of Er^{3+} ion in $MO-WO_3-P_2O_5$ glasses. J. of Physics and Chemistry of Solids, 2003, 64, 1027-1035.

[18] Pisarski W A, Goryczka T, Wodecka-Dus B, Plonska M and Pisarska J. Structure and properties of rare earth-doped lead borate glasses. Mat. Sci. and Engg. B, 2005, 122, 94-99.

[19] Karthikeyan B and Mohan S. Structural, optical and glass transition studies on Nd3+ doped lead bismuth borate glasses. Physica B, 2003, 334, 298-302.

[20] Saritha D, Markandeya Y, Salagram M, Vithal M, Singh A K and Bhikshamaiah G. Effect of Bi_2O_3 on physical, optical and structural studies of $ZnO–Bi_2O_3–B_2O_3$ glasses. J. Non-Cryst. Solids, 2008, 354, 5573-5579.

[21] Raluca Ciceo-Lucacel, Ioan Ardelean. FT-IR and Raman study of silver lead borate-based glasses. J. Non-Cryst. Solids, 2007, 353, 2020-2024.

[22] Rami Reddy M, Bangaru Raju S and Veeraiah N. Acoustic investigations on $PbO-Al_2O_3-B_2O_3$ glasses doped with certain rare earth ions. Bull. Mater. Sci., 2001, 24, 63-68.

[23] Venkateswara Rao P, Satyanarayana T, Srinivasa Reddy Y, Gandhi Y and Veeraiah N. Nickel as a structural probe in $PbO-Bi_2O_3-B_2O_3$ glass system by means of spectroscopic and dielectric studies. Physica B, 2008, 403, 3751-3759.

[24] Jakutis J, Gomes L, Amancio C T, Kassab L R P, Martinelli J R and Wetter N U. Increased Er^{3+} upconversion in tellurite fibers and glasses by co-doping with Yb^{3+}. Optical materials, 2010, 33, 107-111.

[25] Yang G F, Shi D M, Zhang Q Y and Jiang Z H. Spectroscopic properties of Er^{3+}/Yb^{3+} codoped $PbO-Bi_2O_3-Ga_2O_3-Ge_2O_3$ glasses. J. Fluoresc., 2008, 18, 131-137.